Environmental Research Letters

CrossMark

LETTER

The importance of forest structure for carbon fluxes of the Amazon rainforest

Edna Rödig[1,7] , Matthias Cuntz[1,2], Anja Rammig[3,4], Rico Fischer[1], Franziska Taubert[1] and Andreas Huth[1,5,6]

1   UFZ-Helmholtz Centre for Environmental Research, Permoserstr. 15, 04318 Leipzig, Germany
2   INRA, Université de Lorraine, AgroParisTech, UMR Silva, 54000 Nancy, France
3   Technical University of Munich, TUM School of Life Sciences Weihenstephan, Hans-Carl-von-Carlowitz-Platz 2, 85354 Freising, Germany
4   Potsdam-Institute for Climate Impact Research (PIK), Telegraphenberg A62, 14473 Potsdam, Germany
5   University of Osnabrück, Barbarastraße 12, 49076 Osnabrück, Germany
6   German Centre for Integrative Biodiversity Research (iDiv) Halle-Jena-Leipzig, Deutscher Platz 5e, 04103 Leipzig, Germany
7   Author to whom any correspondence should be addressed.

E-mail: edna.roedig@ufz.de

Abstract

Precise descriptions of forest productivity, biomass, and structure are essential for understanding ecosystem responses to climatic and anthropogenic changes. However, relations between these components are complex, in particular for tropical forests.

We developed an approach to simulate carbon dynamics in the Amazon rainforest including around 410 billion individual trees within 7.8 million km^2. We integrated canopy height observations from space-borne LIDAR in order to quantify spatial variations in forest state and structure reflecting small-scale to large-scale natural and anthropogenic disturbances.

Under current conditions, we identified the Amazon rainforest as a carbon sink, gaining 0.56 GtC per year. This carbon sink is driven by an estimated mean gross primary productivity (GPP) of 25.1 tC ha^{-1} a^{-1}, and a mean woody aboveground net primary productivity (wANPP) of 4.2 tC ha^{-1} a^{-1}. We found that successional states play an important role for the relations between productivity and biomass. Forests in early to intermediate successional states are the most productive, and woody above-ground carbon use efficiencies are non-linear. Simulated values can be compared to observed carbon fluxes at various spatial resolutions (>40 m). Notably, we found that our GPP corresponds to the values derived from MODIS. For NPP, spatial differences can be observed due to the consideration of forest successional states in our approach.

We conclude that forest structure has a substantial impact on productivity and biomass. It is an essential factor that should be taken into account when estimating current carbon budgets or analyzing climate change scenarios for the Amazon rainforest.

Introduction

The terrestrial biosphere represents an important, but also an uncertain component of the global carbon cycle (Le Quéré *et al* 2016). In particular, the Amazon rainforest, which accounts for 50% of carbon stored in tropical forests (Pan *et al* 2011), takes a great share of this uncertainty. Estimates on stocks (Mitchard *et al* 2014) and fluxes (Johnson *et al* 2016,

Castanho *et al* 2016) diverge for several reasons. On the one hand, the Amazon shows regional differences in mean wood densities and turnover rates although the drivers are still not entirely understood (Chave *et al* 2006, Malhi *et al* 2006, 2015). On the other hand, the Amazon is exposed to disturbances such as wind blow-downs (Chambers *et al* 2013, Fisher *et al* 2008), droughts (Phillips *et al* 2009, Gatti *et al* 2014), and deforestation (van der Werf *et al* 2009,

Pütz *et al* 2014, Poorter *et al* 2014). Such disturbances shift forests into earlier successional states and influence forests' species composition and structure (Feldpausch *et al* 2011, Dubayah *et al* 2010), factors that are often neglected in large-scale estimates of the carbon budget (Houghton 2005).

In many global vegetation models, net primary productivity is mainly related to the amount of standing biomass (Johnson *et al* 2016). Thereby, models miss out on accounting for the effect of forest structure on productivity. Recent field studies deliver valuable analyses on potential drivers for the spatial variation of biomass and productivity within the Amazon rainforest. It was found that forest dynamics and hence biomass and productivity might be related to seasonality (Chave *et al* 2006, Malhi *et al* 2015, Hofhansl *et al* 2014) or soil properties (soil phosphorus and soil physical properties, Quesada *et al* 2017). It is, however, challenging to derive relations from field studies for large regions as the number and sizes of sample plots may not always be sufficient to be representative of an entire landscape (Marvin *et al* 2014). Analyses of the relation between biomass stocks and climatic conditions in the Amazon are based on ca. 300 one-hectare plots (e.g. Malhi *et al* 2006), and analyses of biomass increments on even less (ca. 200, Brienen *et al* 2015a, 2015b). More detailed analyses on carbon partitioning into gross and net primary production, for example, are based on an even smaller number of plots (e.g. 10 plots in Malhi *et al* 2015). An additional limitation lies in the fact that field studies do not account for the full range of successional states, forest structure, and species composition.

In this study, we present an approach that links a canopy height map with an Amazon-wide forest gap model (Rödig *et al* 2017a). Forest gap models simulate forest succession at the individual tree level. In our regionalization approach, precipitation and clay content of the soil are taken as a proxy for tree mortality which is supported by relations observed in the field (Quesada *et al* 2017). This relation was found to reproduce spatial differences in forest succession (Rödig *et al* 2017a). Spatially variable mortality rates are of particular importance in highly dynamic forests where small-scale mortality events can have a strong effect on forest carbon stocks (Espírito-Santo *et al* 2014). In addition, our forest model simulates forest structure and species compositions throughout all successional states. The linkage with the remotely sensed canopy height map derived from spaceborne LIDAR data (measurements in 2005, Simard *et al* 2011) allows for deriving the current state of the forest at a specific location, considering disturbance at different spatial scales under spatially heterogeneous environmental conditions.

Our approach allows for presenting static maps of carbon fluxes such as gross primary productivity (GPP), above-ground woody net primary productivity (wANPP), and net ecosystem productivity (NEP)

for the Amazon rainforest. Simulation results were compared to previous mean global maps derived from MODIS (Zhao and Running 2010), up-scaled eddy flux measurements FLUXCOM (Jung *et al* 2017, Tramontana *et al* 2016), forest inventories (Malhi *et al* 2015, Brienen *et al* 2015a), and measurements at two eddy-flux towers (FLUXNET, GF-Guy, BR-Sa3). In addition, relations between above-ground biomass (AGB), carbon fluxes, and successional states are explored at various spatial resolutions ($\geq$40 m).

In this study we address the following questions: (a) How do successional states of forests influence the carbon dynamics of the Amazon? (b) How do carbon fluxes vary spatially across the Amazon region? (c) Is the spatial variability of GPP and NPP in the Amazon rainforest mainly driven by standing biomass?
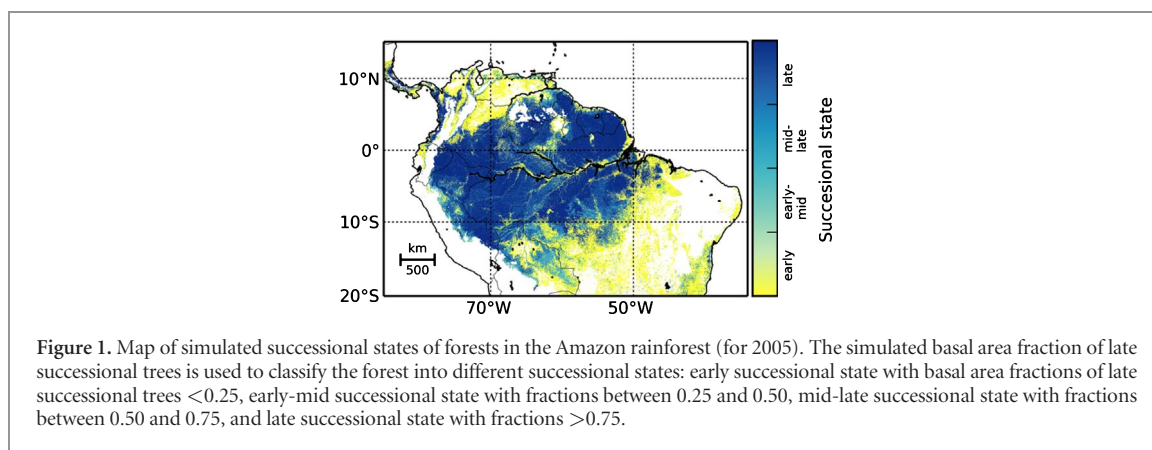
Methods

Study region

The study region covers 7.8 million km^2 of forests in South America that are categorized as rainforest or moist deciduous rainforest (fewer than 5 dry months in which precipitation (mm) $\leq$2 times mean temperature (°C) (FAO 2001)), have an annual mean temperature above 18 °C, are located at an elevation below 1000 m and have an AGB >20 t ha^{-1} (Rödig *et al* 2017a).

An Amazon-wide individual-based forest gap model

Our analyses are based on a regionalized Amazon-wide version (Rödig *et al* 2017a) of the forest gap model FORMIND, which has already been applied at various locations in the tropics (Fischer *et al* 2016). The forest gap model is driven by mean photosynthetic photon flux density (PPFD), mean precipitation (both 0.5°, mean over 2003–2012, Weedon *et al* 2014), and clay fraction of soil (8 km, Wieder *et al* 2014). It simulates forest dynamics at the individual tree level considering the following main processes at a yearly time step: tree growth, competition, establishment, and mortality. Growth of an individual tree depends on its location within the forest community, where trees compete for light and space. A gain in tree biomass results from the difference between photosynthesis and respiration losses. A seedling can establish if light intensity on the forest floor is sufficient.

In our model, tree mortality is an important driver for forest dynamics. Mortality increases when tree crowns are limited in space (crowding). Falling of large trees can damage surrounding trees (gap building) which causes conditional mortality events. In addition, every tree underlies a basic mortality rate which is determined stochastically. The characteristic of the Amazon-wide forest model is that this basic mortality rate varies spatially depending on temporal mean precipitation and the fraction of clay content in soil (Rödig *et al* 2017a). That means that in the model, mortality rates vary in space, but not in time. Hence,

Figure 1. Map of simulated successional states of forests in the Amazon rainforest (for 2005). The simulated basal area fraction of late successional trees is used to classify the forest into different successional states: early successional state with basal area fractions of late successional trees <0.25, early-mid successional state with fractions between 0.25 and 0.50, mid-late successional state with fractions between 0.50 and 0.75, and late successional state with fractions >0.75.

the forest model accounts for regional forest dynamics under mean climate conditions but does not consider inter-annual climate anomalies. Dead biomass is transferred to a dead wood carbon pool from which carbon is constantly transferred to a soil carbon pool (decomposition) or respired to the atmosphere.

The exchange of carbon between the forest and the atmosphere (net ecosystem productivity NEP $[tC\,ha^{-1}\,a^{-1}]$), which is sometimes also referred to as net biome productivity (e.g. Jung *et al* 2011), is described as follows (Paulick *et al* 2017, Sato *et al* 2007):

$$NEP = \sum_{trees} \left(GPP_{tree} - R_{tree} \right) + t_{DA} S_{dead} + t_{SA} S_{slow} + t_{FA} S_{fast}$$

The sum of gross primary productivity (GPP_{tree} $[tC\,ha^{-1}\,a^{-1}]$) minus autotrophic respiration (R_{tree} $[tC\,ha^{-1}\,a^{-1}]$) over all tress equals the woody above-ground NPP (wANPP) of the forest site ($[tC\,ha^{-1}\,a^{-1}]$). Autotrophic respiration R_{tree} is calculated as the sum of maintenance and growth respiration which also includes root respiration (figure S1 available at stacks.iop.org/ERL/13/054013/mmedia). Its annual rate is calculated in order to fit observed above-ground biomass growth of a tree. We assume that wANPP is a constant fraction of NPP (NPP = 2.72wANPP, derived for mature forests from Anderson-Teixeira *et al* 2016). S_{dead} is the dead wood pool, S_{slow} the slow decomposing soil carbon pool and S_{fast} the fast decomposing soil carbon pool (all $[tC\,ha^{-1}]$) with its respiration rates to the atmosphere ($t_{DA} S_{dead}$: to atmosphere, t_{SA}: S_{slow} to atmosphere, t_{FA}: S_{fast} to atmosphere, table S1).

The advantage of simulating each tree individually is that changes in forest structure are captured throughout all different successional states with different species compositions: from bare ground to climax stage including natural tree death. Differences in species composition are represented by three plant functional types: early successional, mid successional and late successional tree types that differ mainly in productivity, light needed at establishment, and mortality rates (table S1). Forest dynamics differ spatially as spatial variable mortality rates cause changes in competition
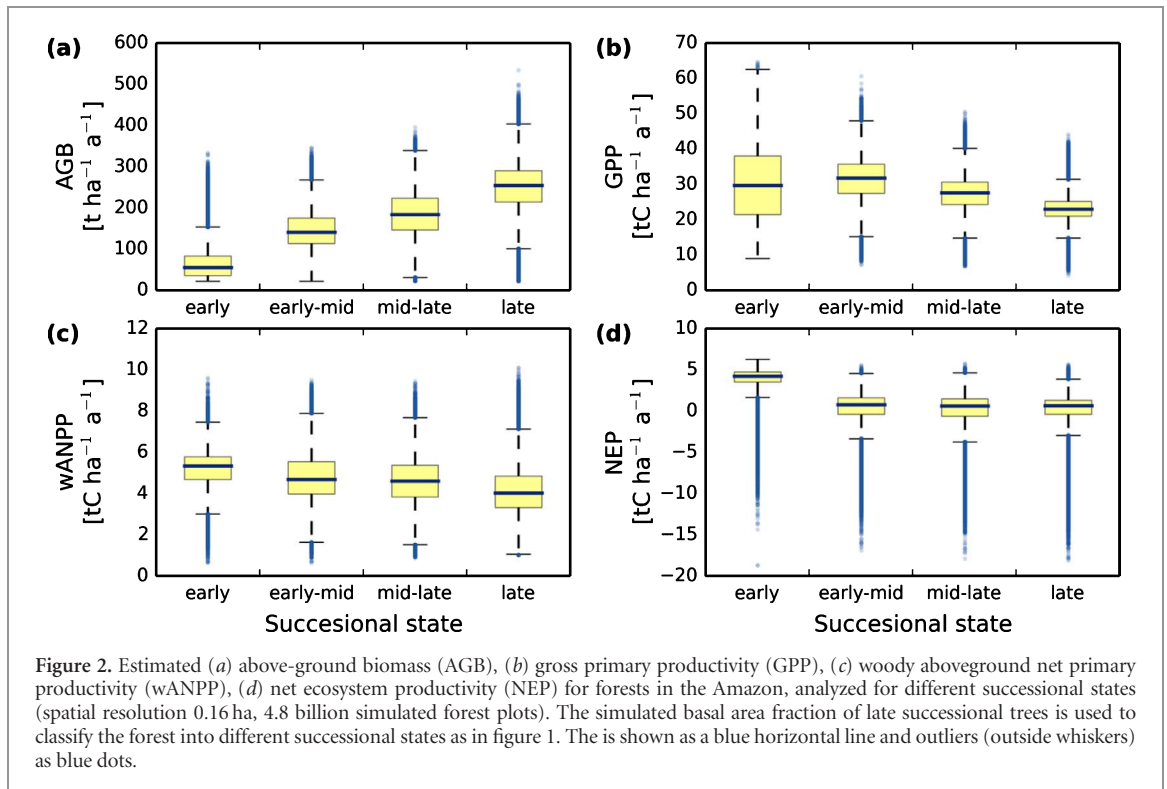
between PFTs. This study focuses on the impact of forest structure on carbon fluxes under mean climatic conditions. This means that tree growth is limited to light and space, but trees grow (in the mean) under mean annual temperature and water conditions.

Technically, the individual-based model could simulate tree growth for every tree in the Amazon rainforest. However, the computational effort can be reduced for areas with similar environmental conditions at 1 km^2 resolution. That means that for every area with similar environmental conditions (in total 1280 areas with similar mean precipitation, mean photosynthetic photon flux density (PPFD), and clay content, Rödig *et al* 2017a), only one model realization on 1 km^2 (100 ha) is performed representatively (figure S2). Our simulation represents 7.8 million km^2 of forest with 410 billion individual trees (>10 cm). Forest succession is simulated over 1000 years from bare ground to climax state (figure S3) on a high-performance Unix cluster.

Identifying the state of the Amazon rainforest
The successional state of each forest site within the Amazon is identified via a canopy height map (Simard *et al* 2011) as in Rödig *et al* (2017a). The canopy height map is based on space-borne LIDAR measurements taken aboard ICESat in May and June 2005. Consequently, the identified successional state of the forests represents the state in 2005. For each location in the Amazon rainforest (1 km^2), we selected the simulated successional states to which the simulated canopy height equals the height given by the canopy height map. A successional state of the forest is here described as the basal area fraction of late successional trees (figure 1). We could then identify the forest's current carbon stock and its associated carbon fluxes (figure S2).

The canopy height map comes with a root mean square error of 6.1 m at 1° resolution (Simard *et al* 2011). We performed an error analysis on how this uncertainty influences simulated GPP, wANPP, and NEP (see supporting information S1). This also includes those uncertainties that result from simulated canopy height and their different identified states. In addition, we tested how fluxes change when keeping

Figure 2. Estimated (*a*) above-ground biomass (AGB), (*b*) gross primary productivity (GPP), (*c*) woody aboveground net primary productivity (wANPP), (*d*) net ecosystem productivity (NEP) for forests in the Amazon, analyzed for different successional states (spatial resolution 0.16 ha, 4.8 billion simulated forest plots). The simulated basal area fraction of late successional trees is used to classify the forest into different successional states as in figure 1. The is shown as a blue horizontal line and outliers (outside whiskers) as blue dots.

the mortality rate constant throughout the Amazon (table S3).

Cross-comparison and validation

We compared our simulation results against observed NPP and GPP values from ten inventory sites in the lowland Amazon rainforest (Malhi *et al* 2015), measured woody above-ground net primary productivity (wANPP) from 193 sites (Brienen *et al* 2015a, 2015b), and GPP and NEP from two eddy covariance sites ($<1\,km^2$ footprint, annual means between 2004–2014, GF-Guy, Bonal *et al* 2008, annual means between 2000–2004, BR-Sa3, Goulden *et al* 2004). Please, note that the eddy covariance method observes the entire net ecosystem exchange (NEE) and we assumed here –NEE = NEP (Chapin *et al* 2006). Global mean GPP and NPP estimates from MODIS at $1\,km^2$ resolution for the years 2000–2010 (Zhao and Running 2010, Running *et al* 2004) and GPP estimates from FLUXCOM at 0.5° resolution for the years 2000–2010 (mean over all realizations of different machine learning methods, Jung *et al* 2017, Tramontana *et al* 2016) were remapped (nearest neighbor, CDO 2015) to the resolution of our map to be compared against our simulation results.

Results

Dynamics of forests in different successional states

By linking vegetation modelling with canopy height map information from remote sensing (Simard *et al* 2011), we were able to derive the successional state of forests in the Amazon rainforest (figure 1), here

as basal area fraction of late successional trees. AGB increases throughout the successional state of a forest as expected (figure 2, figure S5 for additional attributes) while GPP peaks at early-mid successional state and is significantly higher than in mid-late and late successional state. wANPP decreases with successional state of the forest. NEP is significantly higher in early successional than in late successional state. NEP is around 0 in mid-late to late successional state. All fluxes in all states show significant differences (except NEP in mid-late and late successional state).

Spatial distribution of GPP, wANPP and NEP at different spatial scales

Across the Amazon basin, we obtain a mean GPP of forests of $25.1\,tC\,ha^{-1}\,a^{-1}$ (figure 3(*a*), table 1). GPP values are higher along the Amazon river and in the southern Amazon rainforest (figure 3(*a*)). The pattern of woody aboveground productivity (wANPP, figure 3(*b*)) resembles the one of GPP with higher values along the rivers and in the southern Amazon. Mean wANPP is $4.2\,tC\,ha^{-1}\,a^{-1}$. In some parts of the Amazon (e.g. the Guiana Shield), GPP values are higher than the mean while wANPP values are lower than the mean. NEP varies around zero (figure 3(*c*)) with a mean NEP value of $0.7\,tC\,ha^{-1}\,a^{-1}$. NEP values of up to $5\,tC\,ha^{-1}\,a^{-1}$ are reached only along the south-east and north-west.

The variation of GPP, wANPP, and NEP values at small scales (0.16 ha resolution) is higher than the variation at $1\,km^2$ resolution (frequency distributions in figure 3). For example, the analysis of NEP at 0.16 ha resolution shows that forests can release up to $20\,tC\,ha^{-1}\,a^{-1}$ to the atmosphere (figure 2(*d*)), while its

Table 1. Mean ± standard deviation across Amazon rainforest (at 1 km^2 resolution) of gross primary productivity (GPP), net primary productivity (NPP), net ecosystem productivity (NEP), and above-ground biomass (AGB) over 7.8 million km^2 for four sub-regions (according to Feldpausch *et al* 2011, figure S11) derived from three different approaches: FORMIND, MODIS and FLUXCOM.

	FORMIND				MODIS		FLUXCOM
	Mean GPP ± std tC ha^{-1} a^{-1}	Mean NPP ± std tC ha^{-1} a^{-1}	Mean NEP ± std tC ha^{-1} a^{-1}	Mean AGB ± std t ha^{-1}	Mean GPP ± std tC ha^{-1} a^{-1}	Mean NPP ± std tC ha^{-1} a^{-1}	Mean GPP ± std tC ha^{-1} a^{-1}
Western Amazon	24.7 ± 3.0	10.2 ± 2.9	0.7 ± 1.2	208 ± 120	27.9 ± 4.8	13.2 ± 4.6	29.1 ± 6.1
Brazilian Shield	25.6 ± 3.9	12.4 ± 2.7	1.2 ± 1.7	123 ± 112	23.4 ± 3.9	8.5 ± 2.3	25.9 ± 4.8
East Central Amazon	24.7 ± 2.8	11.7 ± 2.3	0.5 ± 1.1	218 ± 86	25.2 ± 2.6	8.8 ± 2.6	30.3 ± 2.1
Guiana Shield	25.0 ± 2.2	10.7 ± 2.7	0.3 ± 0.8	255 ± 93	24.8 ± 2.3	9.9 ± 1.8	31.1 ± 3.1
Amazon region	25.1 ± 3.2	11.3 ± 2.8	0.7 ± 1.4	188 ± 120	25.4 ± 4.2	10.3 ± 3.7	28.8 ± 5.1

maximum release at 1 km^2 is 0.23 tC ha^{-1} a^{-1}. Within an area of 7.8 Mio km^2, the Amazon rainforest takes up 0.56 GtC per year (emissions due to fire and outtake of wood are not included).

Comparison of simulation results with other flux estimates

We compare our obtained values at 1 km^2 resolution (figure 4) with estimates derived from MODIS (1 km^2 resolution, Running *et al* 2004, Zhao and Running 2010), FLUXCOM (0.5° resolution, Jung *et al* 2017, Tramontana *et al* 2016), inventory data (ca. 1 ha plots, Brienen *et al* 2015a, 2015b, Malhi *et al* 2015), and eddy-covariance measurements (<1 km^2 footprint, FLUXNET stations GF-Guy and BR-Sa3).

Gross primary production: The overall frequency distribution of simulated GPP resembles the one derived from MODIS with a mean of 25 tC ha^{-1} a^{-1} (figure 4(*a*)). We observe slightly higher GPP values with MODIS than with our approach for forests in late succession while it seems to be inverse for forests in early succession (figure 5). FLUXCOM GPP is higher with a mean of 28.8 tC ha^{-1} a^{-1}. GPP derived from inventory data (24–42 tC ha^{-1} a^{-1}, Malhi *et al* 2015) and from eddy flux measurements at GF-Guy (32–40 tC ha^{-1} a^{-1}, Bonal *et al* 2008) and BR-Sa3 eddy flux station (29–42 tC ha^{-1} a^{-1}, Goulden *et al* 2004) fall into the upper ranges of our simulated GPP. A one-to-one comparison shows that eddy flux measurements are in rather good agreement with simulation results at the nearest location (figure S8).

Net primary production: MODIS NPP shows a similar pattern as the related GPP distribution and has a clearly defined peak at 9–10 tC ha^{-1} a^{-1} with a mean of 10 tC ha^{-1} a^{-1} (figure 4(*b*)). NPP simulated with FORMIND, on the other hand, is broadly distributed between of 8–16 tC ha^{-1} a^{-1}. In contrast, if the entire region was assumed to be in climax state, there is a single well defined peak in the NPP distribution (figure S9). NPP values derived from forest inventory range from 9–16 tC ha^{-1} a^{-1} (Malhi *et al* 2015). Estimated wANPP from field inventories (Brienen *et al* 2015b) range from 1.1–4.7 tC ha^{-1} a^{-1}, while FORMIND reaches high wANPP values of up to 6 tC ha^{-1} a^{-1} (figure S10). Note that the field inventories are limited to measurements (193 sites) mainly taken in old-grown forests.

Net ecosystem productivity: Simulated NEP values under mean climate conditions fall into the range of recordings at the GF-Guy eddy flux station (1.57 tC ha^{-1} a^{-1}) and the BR-Sa3 station (1.65 tC ha^{-1} a^{-1}).

Relation between analyzed carbon stocks, dynamics and species compositions

Figure 6 shows the obtained relations between carbon fluxes and stocks according to the successional state of a forest plot. Forests in early successional state reach AGB values of 100–150 t ha^{-1}. Forests in early-mid and mid-late successional state reach values up to 300 t ha^{-1}. Forests in late successional state have AGB values greater than 250 t ha^{-1}.

wANPP and AGB stock show a bell-shaped relation (figure 6(*a*)). GPP values and AGB values form a triangle (figure 6(*b*)). Forests in early successional states reach higher GPP values than forests in late successional state (with the same AGB). Comparing both figures (a and b) in late successional states, it is evident that wANPP decreases with increasing AGB while GPP increases with AGB.

The relation between GPP and wANPP displays the woody above-ground carbon use efficiency which varies for different successional states (figure 6(*c*)). Low GPP values are reached for all successional states with a broad range of wANPP values. NEP is always positive for early successional forests, but NEP values of late successional forests show a large variation (figure 6(*d*)).

Error analysis

GPP values in our map come, on average, with a standard error of 4.15 tC ha^{-1} a^{-1} caused by the uncertainties in the canopy height map (figure S6(*b*), table S2). Errors in the GPP map are slightly higher for the Brazilian Shield (including the 'Arc of Deforestation') than for the other regions. wANPP has a mean standard error of 0.90 tC ha^{-1} a^{-1}. Errors in wANPP are highest in East Central Amazon and West Amazon. NEP has an average standard error of 0.65 tC ha^{-1} a^{-1} and is highest for the Brazilian Shield where the error is 23% higher than the overall mean. All fluxes show lower uncertainties for the Guiana Shield.

When keeping mortality rates constant throughout the Amazon, the standard deviations across the Amazon stay more or less constant (table S3).
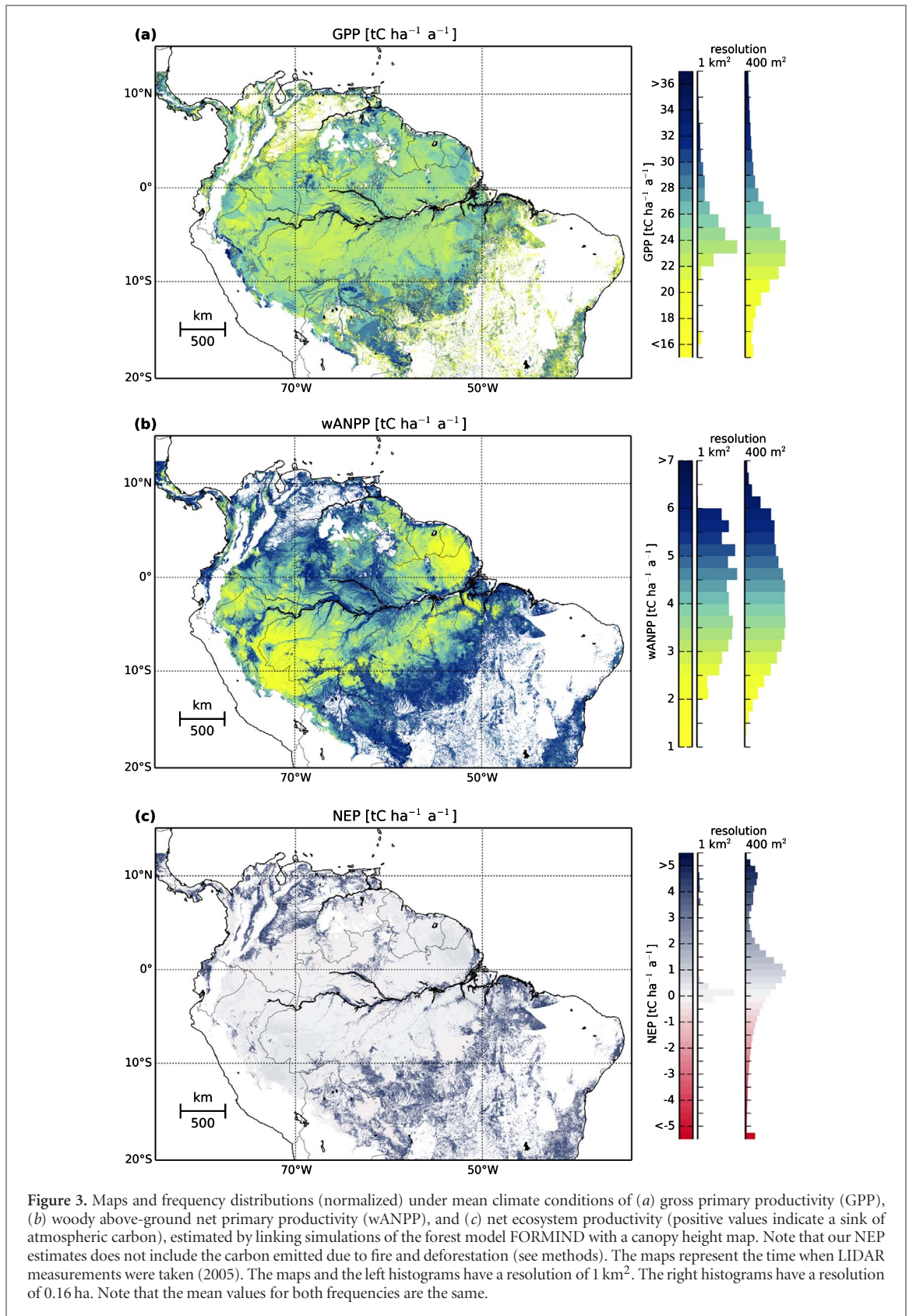
Figure 3. Maps and frequency distributions (normalized) under mean climate conditions of (*a*) gross primary productivity (GPP), (*b*) woody above-ground net primary productivity (wANPP), and (*c*) net ecosystem productivity (positive values indicate a sink of atmospheric carbon), estimated by linking simulations of the forest model FORMIND with a canopy height map. Note that our NEP estimates does not include the carbon emitted due to fire and deforestation (see methods). The maps represent the time when LIDAR measurements were taken (2005). The maps and the left histograms have a resolution of 1 km^2. The right histograms have a resolution of 0.16 ha. Note that the mean values for both frequencies are the same.

Discussion

In this study, we link individual-based simulations with remote sensing measurements to assess the Amazon rainforest's carbon stocks and fluxes.

Carbon fluxes and stocks at different successional states

Our analysis shows how the successional states of a forest (figure 1) influence carbon stocks and fluxes. Noticeably, wANPP, GPP, and NEP are highest for
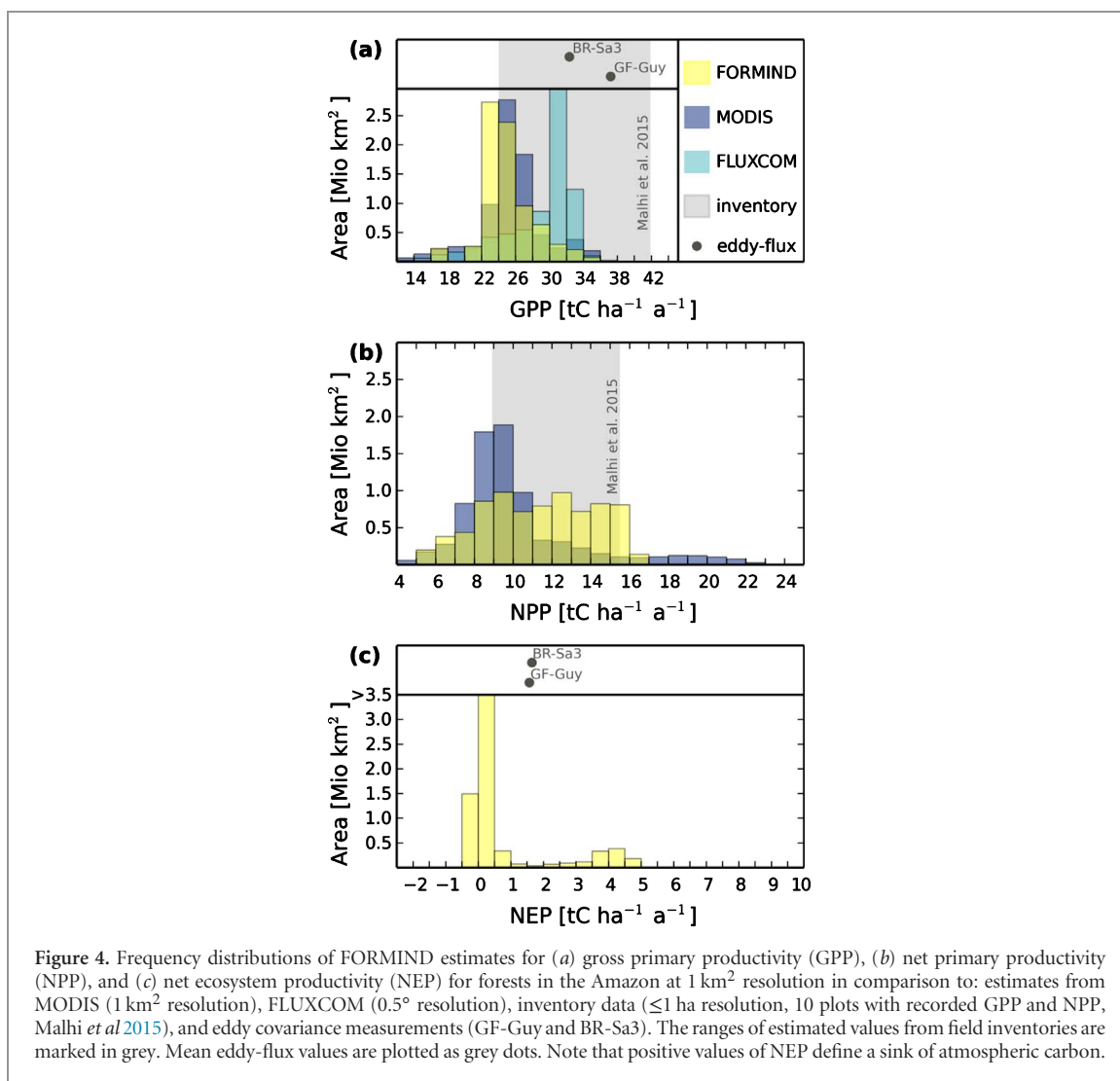
Figure 4. Frequency distributions of FORMIND estimates for (*a*) gross primary productivity (GPP), (*b*) net primary productivity (NPP), and (*c*) net ecosystem productivity (NEP) for forests in the Amazon at 1 km² resolution in comparison to: estimates from MODIS (1 km² resolution), FLUXCOM (0.5° resolution), inventory data (≤1 ha resolution, 10 plots with recorded GPP and NPP, Malhi *et al* 2015), and eddy covariance measurements (GF-Guy and BR-Sa3). The ranges of estimated values from field inventories are marked in grey. Mean eddy-flux values are plotted as grey dots. Note that positive values of NEP define a sink of atmospheric carbon.
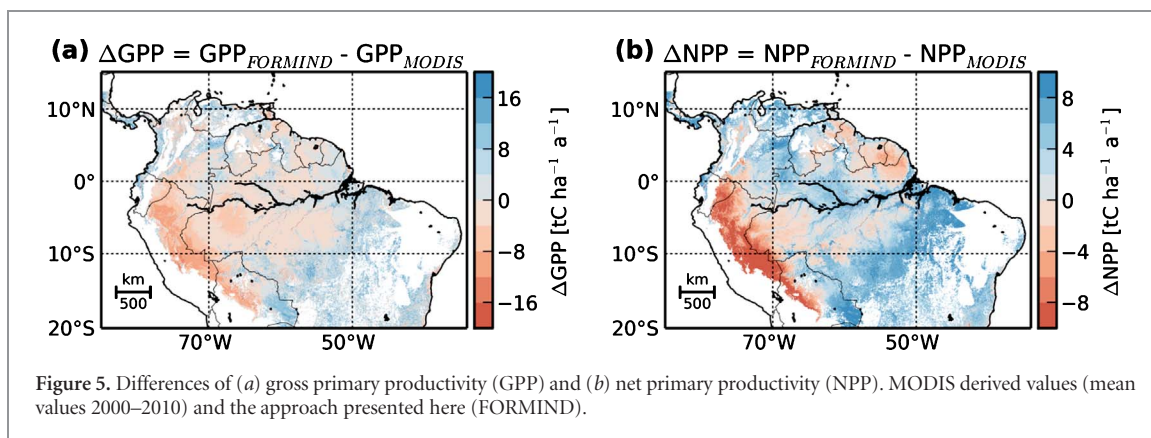
Figure 5. Differences of (*a*) gross primary productivity (GPP) and (*b*) net primary productivity (NPP). MODIS derived values (mean values 2000–2010) and the approach presented here (FORMIND).

forests in early to mid-successional states (figures 2(*c*) and (*d*)). Such forests of high productivity can be found (figure 3), for example, along the 'Arc of deforestation' in the south-east (Nogueira *et al* 2008) where forests are degraded by human activities.

The successional state of a forest is not only influenced by large-scale disturbances, but also by individual tree mortality. This means that even undisturbed,

large forests in mature state consist of different successional states at the small scale (e.g. 400 m², figure S2) and can hence show fluctuations in its carbon dynamics. Chambers *et al* (2013) found, for example, that biomass of a mature forest is stable over time only for sample plots greater than 10 ha. For that reason, derived flux values at small scales show larger variability than at coarser resolution (frequency distributions
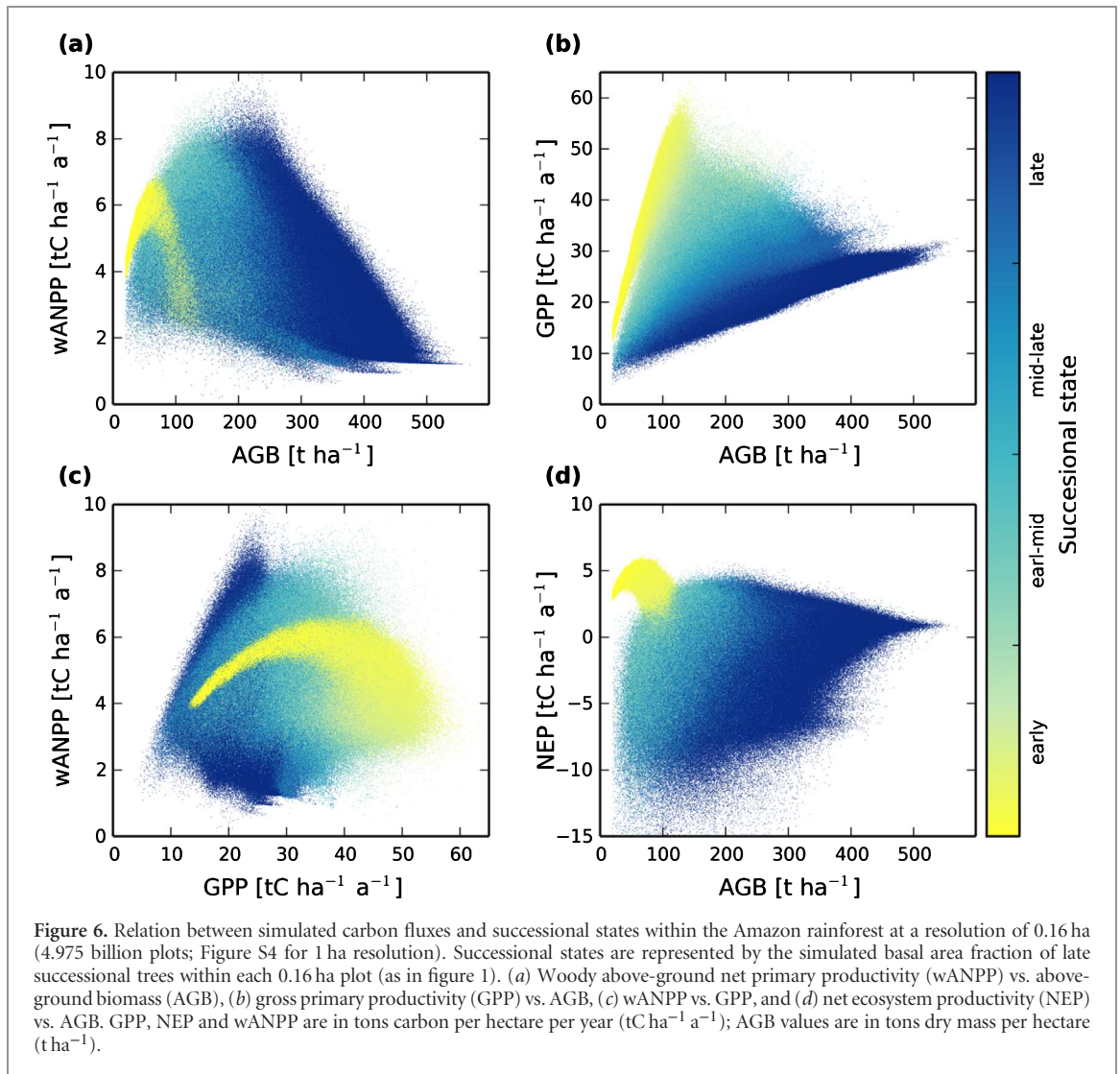
Figure 6. Relation between simulated carbon fluxes and successional states within the Amazon rainforest at a resolution of 0.16 ha (4.975 billion plots; Figure S4 for 1 ha resolution). Successional states are represented by the simulated basal area fraction of late successional trees within each 0.16 ha plot (as in figure 1). (*a*) Woody above-ground net primary productivity (wANPP) vs. above-ground biomass (AGB), (*b*) gross primary productivity (GPP) vs. AGB, (*c*) wANPP vs. GPP, and (*d*) net ecosystem productivity (NEP) vs. AGB. GPP, NEP and wANPP are in tons carbon per hectare per year (tC ha^{-1} a^{-1}); AGB values are in tons dry mass per hectare (t ha^{-1}).

at 400 m^2 = 0.16 ha vs. 1 km^2 resolution in figure 3, and figure 6 vs. Figure S4). This may be related to the finding of Espírito-Santo *et al* (2014) that individual tree mortality over the entire Amazon cause greater biomass losses than large-scale disturbances. Note here that our study includes the consequences of disturbances (regrowth from earlier successional state), but does not account for emissions due to fire or outtake of wood (logging).The relations derived here between simulated stocks and fluxes (figure 6) show that the amount of standing biomass (AGB) is not the only driver for productivity. Our derived relation between wANPP and AGB (figure 6(*a*)) is in agreement with a global field study which reports that highly productive forests may limit AGB values due to a dominance of species with low wood density (Keeling and Phillips 2007). Our relation therefore differs from simulation results of 4 DGVMs for the Amazon region presented in Johnson *et al* (2016). In their study, three DGVMs simulate increasing NPP with increasing AGB. Only one DGVM shows a slight reduction of NPP at high AGB values. They conclude that stem mortality rates need to be included in order to

capture the relation between woody productivity and biomass as observed in the field (Johnson *et al* 2016). In our approach, we explicitly simulate stem mortality which is driven by a spatial variation of precipitation and clay content. As a consequence, spatial differences in dynamics and mean wood density are considered (Rödig *et al* 2017a). This is particularly important for the Amazon where carbon stocks and dynamics are driven by a spatial variation of mortality (Malhi *et al* 2015, Galbraith *et al* 2013, Quesada *et al* 2017, Baker *et al* 2004, Phillips *et al* 2004).

Limitations of our approach

The approach brings along structural uncertainties such as the simplified assumption that NPP is a constant fraction of wANPP, parameter uncertainties, and limitations due to the resolution of input data, here climatological data and the canopy height map (Simard *et al* 2011). The canopy height map is based on discrete LIDAR shots and provides estimates for canopy height at a resolution of 1 km^2. Missing information between shots is a source for uncertainties in the map (Simard *et al* 2011). The

effect these uncertainties on carbon fluxes is discussed below.

We here make simplifications regarding the handling of disturbance histories of the forests (i.e. fire event, logging). Currently, we cannot reconstruct the type of disturbance event from the canopy height map. Consequently, a disturbed forest site is based on the assumption that it either regenerates after deforestation (simulation from bare ground with initialized dead wood and soil pools, table S1), or is influenced by natural tree fall and its resulting mortality (gap-dynamics).

The study presented here focuses on the spatial variability in carbon dynamics resulting from forest structural and environmental differences under current climatic conditions. Consequently, results capture all fluxes for only one point in time (i.e. an average over the period 2003–2012 with structural information of the canopy height map in 2005, Rödig *et al* 2017a). The study design does not yet consider the effects of inter- or intra-annual variations of temperature or atmospheric CO_2 on forest structure (Sakschewski *et al* 2015, Haverd *et al* 2013). It is anticipated to integrate such effects (as it has already been tested for temperate forests in Bohn and Huth 2017 and Rödig *et al.*, 2017) into future work in order to also have the possibility effects of droughts.

Comparison with field data and remote sensing measurements

Testing the representativeness of our GPP map relies on the comparison with other maps derived from remote sensing and simulation (MODIS, Running *et al* 2004, Zhao and Running 2010) and upscaled eddy flux measurements (FLUXCOM, Jung *et al* 2017, Tramontana *et al* 2016). Direct carbon flux measurements in the Amazon rainforest are rare (10 inventory plots (Malhi *et al* 2015) and two eddy flux measurements) and only partly suitable for large-scale estimates.

GPP: The frequency distribution of the MODIS GPP (Running *et al* 2004, Zhao and Running 2010) resembles our simulated GPP distribution (figure 4(*a*)) although both maps are derived from different remote sensing techniques (NDVI vs. LIDAR) which lends confidence to our simulations. MODIS and FLUXCOM show particularly low GPP values for the Brazilian Shield for which FORMIND produces higher GPP values than for the rest of the Amazon (table 1, figure 5). These differences probably arise from the fact that our approach uses a representation of forest succession which leads to higher GPP values in early-mid successional states (figure 2(*b*)). This may also be the reason for differences in GPP values towards the Andes (figure 5, figure S7). In addition, discrepancies may arise from the fact that our approach includes spatial variable mortality rates which lead to differences in forest gap-dynamics across the Amazon. Our simulations at 1 ha resolution reach GPP values

comparable to field observations (figure S4), whereas simulated values at 1 km² are lower.

NPP: Our approach (figure 4(*b*)) displays more forests with high NPP values ($>12\,\mathrm{tC\,ha^{-1}\,a^{-1}}$) than the MODIS product. Please note that the NPP pattern of the MODIS product correlates with its GPP pattern (table 1) whereas our approach indicates forest structure as an important additional factor (GPP vs. NPP, carbon use efficiency is not constant, figure 6(*c*), figure S5(*a*)). We identify two potential explanations for such discrepancy. First, the representation of different PFTs, which allows for simulating forest succession, leads to higher NPP values (figure 2(*c*)), especially in highly disturbed regions like the Brazilian shield (table 1). The successional state identified with the canopy height map seems to have more influence on NPP than internal gap-dynamics due to variable mortality rates (table S3). Second, the MODIS product, which is often used for global estimates (Jung *et al* 2017, Bloom *et al* 2016, Zhao and Running 2010), is limited by the fact that it is derived from Normalized Difference Vegetation Index (NDVI) values. The NDVI tends to saturate in dense mature forests and, thus, has limited capability to identify spatial variations, such as in the Amazon (Hall *et al* 2011, Myneni *et al* 2001). The method presented here uses a canopy height map (Simard *et al* 2011) that is derived from LIDAR measurements. Active remote sensing tracers (here LIDAR) have the advantage that they are highly sensitive to structural variations (Lefsky *et al* 2002).

NEP: We here estimate that the Amazon forest gains, on average, 0.56 Gt of carbon per year and as such yields a positive NEP. Even when considering a mean standard error of ±0.51 Gt of carbon per year due to uncertainties in the canopy height map, the Amazon is identified as a sink of atmospheric carbon. As this value is the potential carbon uptake due to the successional states of the forests, our estimate compensates approximately the amount of carbon currently released due to deforestation and land-use change in South America (Baccini *et al* 2012). In particular, forests in earlier successional states contribute to an uptake of atmospheric carbon (Poorter *et al* 2014, figure 2(*d*)).

Conclusion

In our study, we have shown that the successional state of forests, and hence forest structure and species composition, have a strong effect on NPP and NEP. This effect is reflected in higher NEP and wANPP values for forests that regrow after deforestation (Poorter *et al* 2014), particularly, along the Arc of deforestation and higher wANPP values in East-central Amazon due to internal gap-dynamics. Our results reveal that NEP across the Amazon is a carbon sink of 0.56 ± 0.51 Gt C per year driven by high productivity in regenerating forest areas, approximately offsetting

estimates of fire and deforestation emissions. We show that AGB alone does not account for productivity differences (figure 6) and found that structure and species compositions are important as well.

Individual-based modelling at the large scale, such as the Amazon rainforest, is expensive in computational demand. However, a high-resolution approach allows for integrating observational data at different spatial scales and contributes to a better understanding of forest dynamics at the large scale. The approach can be expanded in future work by integrating further remote sensing data into the analysis. For example, matching vertical canopy profiles from LIDAR with simulated profiles (Knapp *et al* 2018) can provide additional insights into the actual successional state of forests. Our analyses highlight the importance of accounting for forest structure when simulating carbon dynamics. We therefore suggest that forest structure should also be incorporated in global dynamic vegetation modelling.

Acknowledgments

ORCID iDs

Edna Rödig https://orcid.org/0000-0002-6248-8844

References

Anderson-Teixeira K J, Wang M M H, Mcgarvey J C and Lebauer D S 2016 Carbon dynamics of mature and regrowth tropical forests derived from a pantropical database (TropForC-db) *Glob. Change Biol.* **22** 1690–709

Baccini A *et al* 2012 Estimated carbon dioxide emissions from tropical deforestation improved by carbon-density maps *Nat. Clim. Change* **2** 182–5

Baker T R *et al* 2004 Variation in wood density determines spatial patterns in Amazonian forest biomass *Glob. Change Biol.* **10** 545–62

Bloom A A, Exbrayat J-F, van der Velde I R, Feng L and Williams M 2016 The decadal state of the terrestrial carbon cycle: global retrievals of terrestrial carbon allocation, pools, and residence times *Proc. Natl Acad. Sci.* **113** 1285–90

Bohn F J and Huth A 2017 The importance of forest structure to biodiversity–productivity relationships *R. Soc. Open Sci.* **4** 160521

Bonal D *et al* 2008 Impact of severe dry season on net ecosystem exchange in the Neotropical rainforest of French Guiana *Glob. Change Biol.* **14** 1917–33

Brienen R J W *et al* 2015a Long-term decline of the Amazon carbon sink *Nature* **519** 344–8

Brienen R J W *et al* 2015b Plot data from: 'Long-term decline of the Amazon carbon sink' *ForestPlots.NET* (10.5521/Forest Plots.net/2014_4)

Castanho A D A, Galbraith D, Zhang K, Coe M T, Costa M H and Moorcroft P 2016 Changing Amazon biomass and the role of atmospheric CO_2 concentration, climate, and land use *Glob. Biogeochem. Cycles* **30** 18–39

CDO 2015 CDO 2015: Climate Data Operators (www.mpimet. mpg.de/cdo)

Chambers J Q, Negron-Juarez R I, Marra D M, Di Vittorio A, Tews J, Roberts D, Ribeiro G H P M, Trumbore S E and Higuchi N 2013 The steady-state mosaic of disturbance and succession across an old-growth Central Amazon forest landscape *Proc. Natl Acad. Sci.* **110** 3949–54

Chapin F S *et al* 2006 Reconciling carbon-cycle concepts, terminology, and methods *Ecosystems* **9** 1041–50

Chave J, Muller-Landau H C, Baker T R, Easdale T A, ter Steege H and Webb C O 2006 Regional and phylogenetic variation of wood density across 2456 Neotropical tree species *Ecol. Appl.* **16** 2356–67

Dubayah R O, Sheldon S L, Clark D B, Hofton M A, Blair J B, Hurtt G C and Chazdon R L 2010 Estimation of tropical forest height and biomass dynamics using lidar remote sensing at la Selva, Costa Rica *J. Geophys. Res. Biogeosci.* **115** 1–17

Espírito-Santo F D B B *et al* 2014 Size and frequency of natural forest disturbances and the Amazon forest carbon balance *Nat. Commun.* **5** 1–6

FAO 2001 Global Forest Resources Assessment

Feldpausch T R *et al* 2011 Height-diameter allometry of tropical forest trees *Biogeosciences* **8** 1081–106

Fischer R *et al* 2016 Lessons learned from applying a forest gap model to understand ecosystem and carbon dynamics of complex tropical forests *Ecol. Modell.* **326** 124–33

Fisher J I, Hurtt G C, Thomas R Q and Chambers J Q 2008 Clustered disturbances lead to bias in large-scale estimates based on forest sample plots *Ecol. Lett.* **11** 554–63

Galbraith D *et al* 2013 Residence times of woody biomass in tropical forests *Plant Ecol. Divers.* **6** 139–57

Gatti L V *et al* 2014 Drought sensitivity of Amazonian carbon balance revealed by atmospheric measurements *Nature* **506** 76–80

Goulden M L, Miller S D, da Rocha H R, Menton M C, de Freitas H C, e Silva Figueira A and de Sousa C A D 2004 Diel and seasonal patterns of tropical forest CO_2 exchange *Ecol. Appl.* **14** 42–54

Hall F G *et al* 2011 Characterizing 3D vegetation structure from space: mission requirements *Remote Sens. Environ.* **115** 2753–75

Haverd V, Smith B, Cook G D, Briggs P R, Nieradzik L, Roxburgh S H, Liedloff A, Meyer C P and Canadell J G 2013 A stand-alone tree demography and landscape structure module for Earth system models *Geophys. Res. Lett.* **40** 5234–9

Hofhansl F, Schnecker J, Singer G and Wanek W 2014 New insights into mechanisms driving carbon allocation in tropical forests *New Phytol.* **2014** 137–46

Houghton R A 2005 Aboveground forest biomass and the global carbon balance *Glob. Change Biol.* **11** 945–58

Johnson M O *et al* 2016 Variation in stem mortality rates determines patterns of above-ground biomass in Amazonian forests: implications for dynamic global vegetation models *Glob. Change Biol.* **22** 3996–4013

Jung M *et al* 2011 Global patterns of land-atmosphere fluxes of carbon dioxide, latent heat, and sensible heat derived from eddy covariance, satellite, and meteorological observations *J. Geophys. Res. Biogeosciences* **116** 1–16

Jung M *et al* 2017 Compensatory water effects link yearly global land CO_2 sink changes to temperature *Nature* **541** 516–20

Keeling H C and Phillips O L 2007 The global relationship between forest productivity and biomass *Glob. Ecol. Biogeogr.* **16** 618–31

Knapp N, Fischer R and Huth A 2018 Linking lidar and forest modeling to assess biomass estimation across scales and disturbance states *Remote Sens. Environ.* **205** 199–209

Lefsky M A, Cohen W B, Parker G G and Harding D J 2002 Lidar remote sensing for ecosystem studies *Bioscience* **52** 19–30

Malhi Y *et al* 2015 The linkages between photosynthesis, productivity, growth and biomass in lowland Amazonian forests *Glob. Change Biol.* **21** 2283–95

Malhi Y *et al* 2006 The regional variation of aboveground live biomass in old-growth Amazonian forests *Glob. Change Biol.* **12** 1107–38

Marvin D C, Asner G P, Knapp D E, Anderson C B, Martin R E, Sinca F and Tupayachi R 2014 Amazonian landscapes and the bias in field studies of forest structure and biomass *Proc. Natl Acad. Sci. USA* **111** E5224–32

Mitchard E T A *et al* 2014 Markedly divergent estimates of Amazon forest carbon density from ground plots and satellites *Glob. Ecol. Biogeogr.* **23** 935–46

Myneni R B, Dong J, Tucker C J, Kaufmann R K, Kauppi P E, Liski J, Zhou L, Alexeyev V and Hughes M K 2001 A large carbon sink in the woody biomass of Northern forests *Proc. Natl Acad. Sci. USA* **98** 14784–9

Nogueira E M, Nelson B W, Fearnside P M, França M B and Ade Oliveira Á C 2008 Tree height in Brazil's 'arc of deforestation': shorter trees in south and southwest Amazonia imply lower biomass *Forest Ecol. Manage.* **255** 2963–72

Pan Y *et al* 2011 A large and persistent carbon sink in the world's forests *Science* **333** 988–93

Paulick S, Dislich C, Homeier J, Fischer R and Huth A 2017 The carbon fluxes in different successional stages: modelling the dynamics of tropical montane forests in South Ecuador *Forest Ecosyst.* **4** 5

Phillips O L *et al* 2009 Drought sensitivity of the Amazon rainforest *Science* **323** 1344–7

Phillips O L *et al* 2004 Pattern and process in Amazon tree turnover, 1976–2001 *Phil. Trans. R. Soc. B Biol. Sci.* **359** 381–407

Poorter L *et al* 2014 Long-term carbon loss in fragmented Neotropical forests *Nat. Commun.* **5** 5037

Pütz S, Groeneveld J, Henle K, Knogge C, Martensen A C, Metz M, Metzger J P, Ribeiro M C, de Paula M D and Huth A 2014 Long-term carbon loss in fragmented Neotropical forests *Nat. Commun.* **5** 5037

Le Quéré C *et al* 2016 Global carbon budget 2016 *Earth Syst. Sci. Data* **8** 605–49

Quesada C A *et al* 2017 Spatial heterogeneity of biomass and forest structure of the Amazon rain forest: Linking remote sensing, forest modelling and field inventory *Glob. Ecol. Biogeogr.* **26** 1292–302

Rödig E, Cuntz M, Heinke J, Rammig A and Huth A 2017a Spatial heterogeneity of biomass and forest structure of the Amazon rain forest: linking remote sensing, forest modelling and field inventory *Glob. Ecol. Biogeogr.* **26** 1292–302

Rödig E, Huth A, Bohn F, Rebmann C and Cuntz M 2017 Estimating the carbon fluxes of forests with an individual-based forest model *Forest Ecosyst.* **4** 4

Running S W, Nemani R R, Heinsch F A, Zhao M, Reeves M and Hashimoto H 2004 A continuous satellite-derived measure of global terrestrial primary production *Bioscience* **54** 547

Sato H, Itoh A and Kohyama T 2007 SEIB–DGVM: a new Dynamic Global Vegetation Model using a spatially explicit individual-based approach *Ecol. Modell.* **200** 279–307

Sakschewski B, von Bloh W, Boit A, Rammig A, Kattge J, Poorter L, Penuelas J and Thonicke K 2015 Leaf and stem economics spectra drive diversity of functional plant traits in a dynamic global vegetation model *Glob. Change Biol.* **21** 2711–25

Simard M, Pinto N, Fisher J B and Baccini A 2011 Mapping forest canopy height globally with spaceborne lidar *J. Geophys. Res.* **116** G04021

Tramontana G *et al* 2016 Predicting carbon dioxide and energy fluxes across global FLUXNET sites with regression algorithms *Biogeosciences* **13** 4291–313

Weedon G P, Balsamo G, Bellouin N, Gomes S, Best M J and Viterbo P 2014 The WFDEI meteorological forcing data set: WATCH Forcing Data methodology applied to ERA-Interim reanalysis data *Water Resour. Res.* **50** 7505–14

van der Werf G R, Morton D C, DeFries R S, Olivier J G J, Kasibhatla P S, Jackson R B, Collatz G J and Randerson J T 2009 CO_2 emissions from forest loss *Nat. Geosci.* **2** 737–8

Wieder W R, Boehnert J, Bonan G B and Langseth M 2014 *Regridded Harmonized World Soil Database v1.2. Data Set* (Oak Ridge, TN: Oak Ridge National Laboratory Distributed Active Archive Center) (https://doi.org/10.3334/ORNLDAAC/1247)

Zhao M and Running S W 2010 Drought-induced reduction in global *Science* **329** 940–3